ELSEVIER

Surface Science 464 (2000) 183–192

surface science

www.elsevier.nl/locate/susc

Investigation of the surface chemistry of crown ethers: the adsorption and reaction of 1,4-dioxane on palladium (111)

S. Azad, D.W. Bennett, W.T. Tysoe *

Department of Chemistry and Laboratory for Surface Studies, University of Wisconsin–Milwaukee, Milwaukee, WI 53211, USA

Received 31 January 2000; accepted for publication 1 June 2000

Abstract

1,4-Dioxane adsorbs on Pd(111) at 80 K to form an overlayer saturating at an exposure of ~4 L (1 L = 1×10^{-6} Torr s) and desorbs with a peak centered at ~268 K in temperature-programmed desorption. Multilayer growth commences for exposures >2 L suggesting that they form before the monolayer is completed. The multilayers desorb at ~160 K. Reflection–absorption infrared spectroscopy of both normal and perdeuterated dioxane suggests that it converts from its usual chair conformation in the gas phase into a boat conformation in the monolayer, allowing the lone pairs on both oxygen atoms to interact with the surface. A portion of the adsorbed dioxane thermally decomposes at or below ~300 K to desorb ethylene and hydrogen and to deposit CO onto the surface. The adsorbed CO thermally desorbs at ~460 K.

Keywords: Chemisorption; Ethers; Infrared absorption spectroscopy; Palladium; Surface chemical reaction; Thermal desorption spectroscopy

1. Introduction

The notion of 'self-assembly' has been applied over the past few years both to the construction of large molecular assemblies and supramolecular arrays [1]. Ordered 'self-assembled' monolayers have been grown on surfaces where self-assembly into ordered arrays is driven by the intermolecular van der Waals interactions between the long, anchored chains [2–12]. Large assemblies of organic molecules have been synthesized that comprise interlocking molecules. Examples of these include catananes, which consist of interlocking ring molecules that form chains in which the cyclic molecules form the links [13–17], and rotaxanes, where rings are trapped on the spindles of dumbbell-shaped molecules [18–25]. Variants of these molecules, pseudorotaxanes, have been fabricated in which the spindle is not locked in place by the presence of large terminal groups but is merely threaded through the center of the cyclic molecule [26,27].

Many of the synthetic strategies for these types of molecule have exploited template-directing interactions, such as van der Waals forces (as in the case of self-assembled monolayers above), hydrogen or donor–acceptor bonds. Crown ethers provide a classical example of such interactions. These were discovered in the 1960s [28] and comprise polycyclic molecules with the general formula $(CH_2OCH_2)_n$ and are named 3*n*-crown-*n*, where each of the *n* oxygen atoms is bound between two carbon atoms arranged in a ring consisting of 3*n* (either oxygen or carbon) atoms. An important

* Corresponding author. Fax: +1-414-229-5036.
E-mail address: wtt@csd.uwm.edu (W.T. Tysoe)

0039-6028/00/$ - see front matter
PII: S0039-6028(00)00661-0

characteristic of their chemistry is the complexation by the ether oxygen atoms of various ionic species; this furnishes a simple example of 'host–guest' chemistry and is used as a simple model for analogous biological interactions, where the crown ether acts as the host and cationic species as the guest [29–31]. This chemistry also has the potential to provide a strategy for selectively removing cationic species from water. Crown ethers have recently been reacted with dialkyl ammonium ions to synthesize pseudorotaxanes [23].

In order to attempt to exploit such host–guest chemistry in the heterogeneous phase, we have embarked on an investigation of the chemistry of crown ethers on surfaces. One goal, ultimately, is to synthesize self-assembling systems using adsorbed crown ethers of various sizes to form surface rotaxanes where adsorbate molecules penetrate the orifice of the crown ether ring to form an ordered system. Varying the radius of the crown ether ring also might provide a method of restricting the size of ensembles of metal atoms available at the surface and provide a strategy for modifying the sites available for a surface (catalytic) reaction.

Palladium was selected as an appropriate substrate for these investigations for various reasons. First, it is sufficiently reactive that crown ethers are likely to adsorb without undergoing facile thermal decomposition. Second, palladium catalyzes an array of reactions with different ensemble requirements in ultrahigh vacuum, from acetylene cyclotrimerization on the one hand, which requires a relatively large ensemble of palladium atoms to proceed [32], to ethylene or acetylene hydrogenation, on the other hand, with only modest ensemble requirements [33]. This investigation has been initiated by studying conceptually the simplest crown ether, 1,4-dioxane, which, using the nomenclature described above, is 6-crown-2. Although this is not conventionally thought of as a crown ether, it is the smallest member of the homologous series and, as such, is likely to be the simplest to understand.

2. Experimental

The experiments were carried out in two stainless-steel, ultrahigh vacuum chambers operating at base pressures of 1×10^{-10} Torr following bakeout and which have been described in detail elsewhere [34,35]. Infrared data were collected from a palladium single crystal sample mounted in a modified 2.75″ six-way cross equipped with infrared-transparent KBr windows. The sample could be resistively heated to 1200 K or cooled to 80 K using liquid nitrogen. Light from a Midac model M2000 infrared spectrometer passes through a polarizer and is focused onto the sample at an incidence angle of $\sim 80^{\circ}$ and the reflected light steered onto the detector of a liquid-nitrogen-cooled, mercury cadmium telluride detector. The complete light path is enclosed and purged with dry, CO_2-free air. The spectrometer is controlled using SpectraCalc software typically operated at 4 cm^{-1} resolution and data were typically collected for 1000 scans.

In the second chamber, the sample was mounted to a carousel-geometry manipulator and could similarly be resistively heated to 1200 K and cooled to 80 K by thermal contact to a liquid-nitrogen-filled reservoir. Temperature-programmed desorption data were collected using a heating rate of ~ 7 K/s and desorbing species detected using a Dichor quadrupole mass spectrometer interfaced to a PC allowing five masses to be monitored sequentially during the same desorption sweep. In this case the sample was dosed via a tube, which minimized background contamination and dosing of the supports. This gave a pressure enhancement compared with the background pressure of ~ 58. In order to minimize spurious signals further, the mass spectrometer is enclosed in a shroud with a 1 cm diameter hole in the front.

The sample is cleaned using a standard procedure, which consists of heating at 1000 K in $\sim 4 \times 10^{-8}$ Torr of oxygen and annealing at 1200 K in vacuo to remove any remaining oxygen. Since the carbon KLL Auger feature is effectively obscured by a strong palladium peak, Auger spectroscopy is not particularly sensitive to the presence of small amounts of carbon on the surface. It was found that a more sensitive gauge of carbon coverage was to saturate the surface with oxygen and to perform a temperature-programmed desorption experiment. The presence of surface carbon is manifested by the desorption of CO. As

the surface becomes depleted of carbon, the CO yield decreases and the yield of oxygen increases correspondingly. The complete absence of carbon is indicated by the desorption of only O_2.

The 1,4-dioxane (Aldrich, 99+%) and d_8-dioxane (Aldrich, 99 at.%) used for these experiments were transferred to glass vials and further purified by repeated freeze–pump–thaw cycles and their cleanliness monitored mass spectroscopically.

3. Results

Temperature-programmed desorption spectra taken monitoring 88 amu, which is uniquely due to the desorption of dioxane from the surface, are displayed in Fig. 1 as a function of exposure. At lower exposures, the spectrum exhibits a single peak centered at 268 K corresponding to desorption of dioxane adsorbed in the first layer. This peak is somewhat asymmetric, with a tail that extends to ~450 K. As the exposure increases to 1.16 L (1 L = 1×10^{-6} Torr s), a peak appears at ~144 K that moves to slightly higher temperatures as the exposure increases, and so appears at 158 K at an exposure to 4.64 L. Note that exposures are not corrected for ionization gauge sensitivities. The 268 K peak grows with increasing exposure and the peak temperature remains constant at 268 K, although the tail to higher temperature becomes more evident. Fig. 2 shows a plot of the peak area for each of these desorption states as a function of exposure. This reveals that the 158 K peak (●) starts to grow before the 268 K feature (■) has saturated in intensity. The 158 K peak continues to grow with increasing exposure and is therefore assigned to adsorption into second and subsequent layers. This temperature is in good agreement with that found for multilayers of 1,4-dioxane desorbing

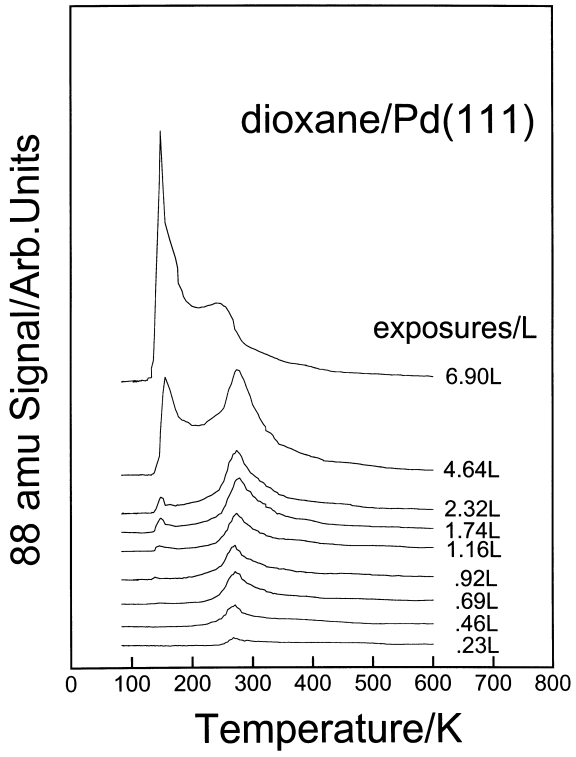

Fig. 1. The 88 amu (dioxane) temperature-programmed desorption spectra following adsorption of dioxane on Pd(111) at 80 K as a function of exposures. The exposures are marked adjacent to each spectrum and are uncorrected for ionization gauge sensitivity.

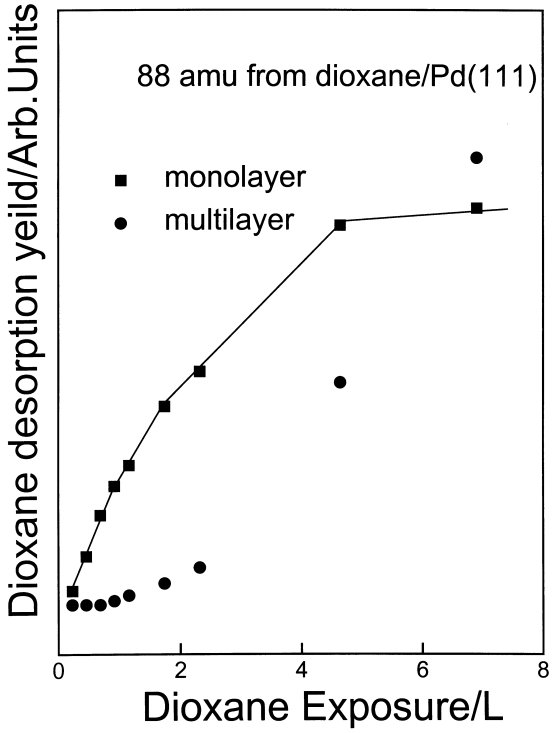

Fig. 2. Plot of the yield from the 268 and 158 K desorption states as a function of exposure.

from Ag(110) [36] and Ru(001) [37]. In contrast, the intensity of the 268 K feature saturates at an exposure of ~4 L and is therefore assigned to desorption from the first monolayer. The results in Fig. 2 also indicate that the second layer forms before the completion of the first.

Fig. 3 displays a corresponding series of temperature-programmed desorption data as a function of dioxane exposure monitoring 28 amu. This is a fragment of dioxane and shows the low-temperature feature at between 145 and 158 K as well as the broad 268 K peak, both seen in Fig. 1. Also evident as a shoulder on the 268 K peak is a feature at 312 K and a peak that grows with increasing exposure at 460 K. In order to establish the desorbing molecules producing these features, temperature-programmed desorption data were collected at 15, 26, 27 and 28 amu for a dioxane exposure of 1.04 L (Fig. 4). The 460 K state has intensity only at 28 amu, with no signal appearing in these spectra at 15, 26 or 27 amu. This indicates that the 460 K feature is due to CO desorption. The intensities of the sharp, low-temperature (~150 K) peak, as well as the 268 K feature at these masses, agree well with the mass spectrometer ionizer fragmentation pattern of dioxane, thus confirming that these features are due to dioxane desorption. The feature at 312 K is more clearly evident in these spectra and has intensity at 26 and 27 amu but none at 15 amu, indicating that this peak is not due to dioxane desorption. The fragmentation pattern agrees well with that for ethylene and is assigned to some desorption of ethylene from the surface. Similar spectra collected with other dioxane exposures confirm this conclusion. Finally, Fig. 5 shows the 2 and 4 amu spectra following adsorption of d_8-dioxane (1.16 L) onto

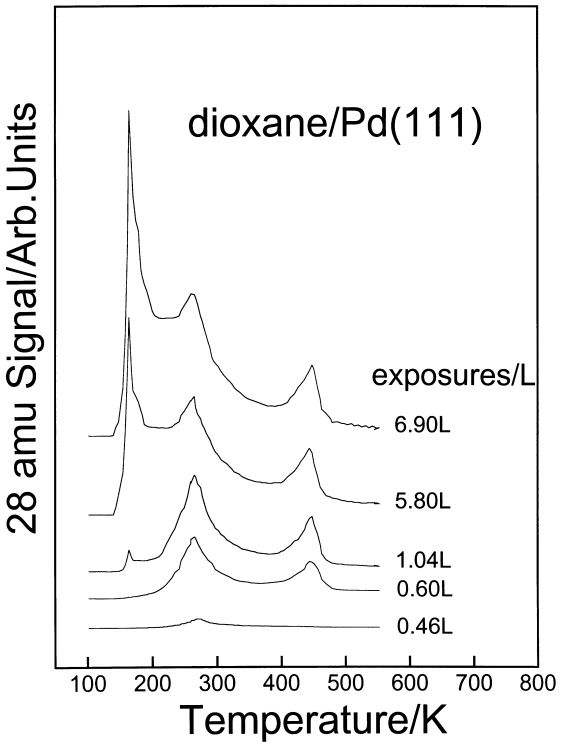

Fig. 3. The 28 amu (dioxane, CO and ethylene; see text) temperature-programmed desorption spectra following adsorption of dioxane on Pd(111) at 80 K as a function of exposures. The exposures are marked adjacent to each spectrum and are uncorrected for ionization gauge sensitivity.

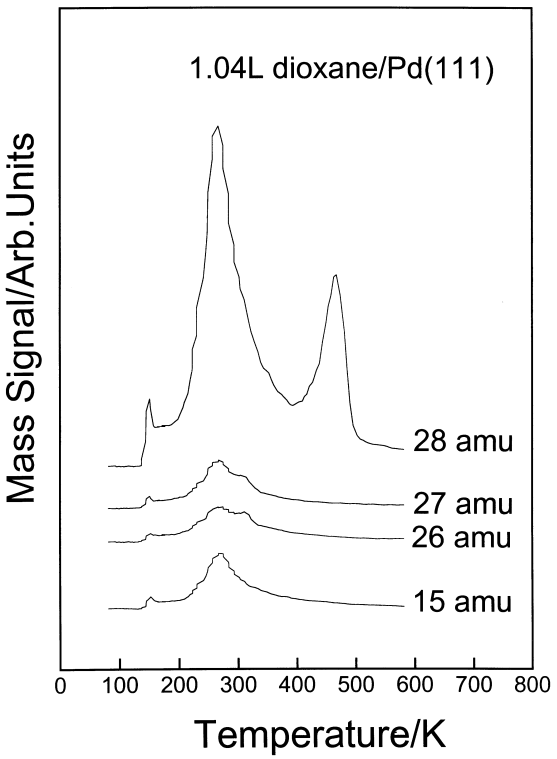

Fig. 4. Temperature-programmed desorption spectra taken after a 1.04 L exposure of dioxane to Pd(111) at 80 K measured at 28, 27, 26 and 15 amu. Exposures are uncorrected for ionization gauge sensitivity.

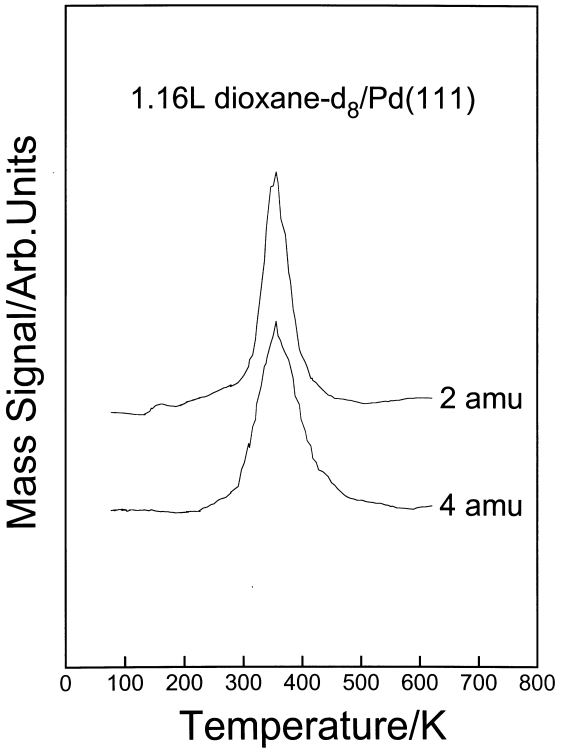

Fig. 5. The 2 and 4 amu (D_2) temperature-programmed desorption spectra following a 1.16 L exposure of d_8-dioxane to Pd(111) at 80 K. Exposures are uncorrected for ionization gauge sensitivity.

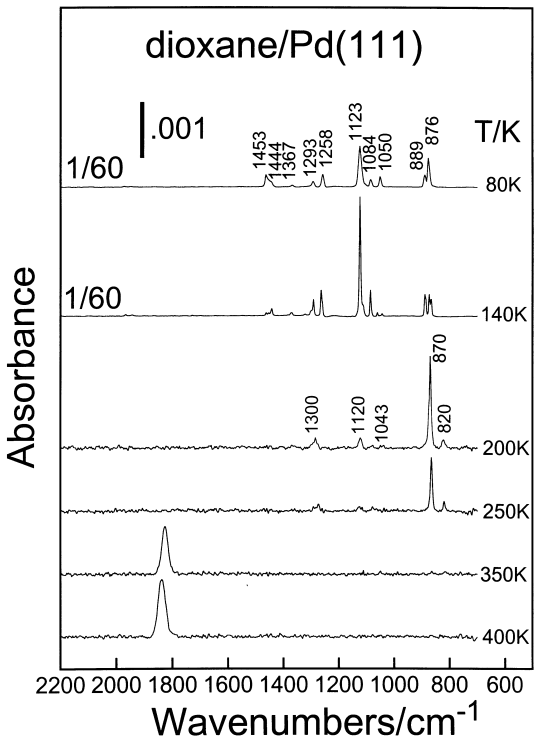

Fig. 6. Reflection–absorption infrared spectra of a multilayer of dioxane adsorbed on Pd(111) at 80 K and annealed to various temperatures. The annealing temperatures are marked adjacent to the corresponding spectrum and the absorbance scale is marked as a vertical line on the figure.

the surface corresponding to the desorption of deuterium at 355 K. Perdeutero-dioxane was used for this experiment to eliminate signals due to any hydrogen desorption due to background adsorption to ensure that the hydrogen arose only from dioxane. No other desorbing species was detected.

The infrared spectra are shown in Fig. 6 (for d_0-dioxane) and Fig. 7 (for d_8-dioxane) after condensing dioxane multilayers on the surface in each case. Both of these multilayer spectra agree very well with the corresponding gas-phase frequencies [38] and the assignments are summarized in Tables 1 and 2. Shoulders are also evident at slightly higher frequencies on the 1105 and 1038 cm^{-1} peaks, and these will be discussed in greater detail below. The spectra that appear after heating to 140 K are shown also in Figs. 6 and 7. These exhibit features that are in good agreement with the condensed multilayer, except that they are much better resolved so that, for example, the CD_2 stretching modes that appear as a single peak at 80 K are well resolved into two features at 2098 and 2083 cm^{-1} after heating to 140 K. This may be indicative of some degree of order in the second and subsequent layers caused by annealing the sample. In addition to features that correspond well to gas-phase dioxane, extra relatively weak peaks are seen at 1300, 1120, 1043, 870 and 820 cm^{-1} following the adsorption of d_0-dioxane and at 1140, 1082, 1030, 890, 757 and 740 cm^{-1} in the case of d_8-dioxane adsorption. These are relatively close to, but distinctly different from, the peaks due to the condensed layer. The spectra change drastically on heating to 200 K [corresponding to completion of the low-temperature ($\sim$150 K) desorption state] but close to the onset of the 268 K desorption state (Figs. 1, 3 and 4).

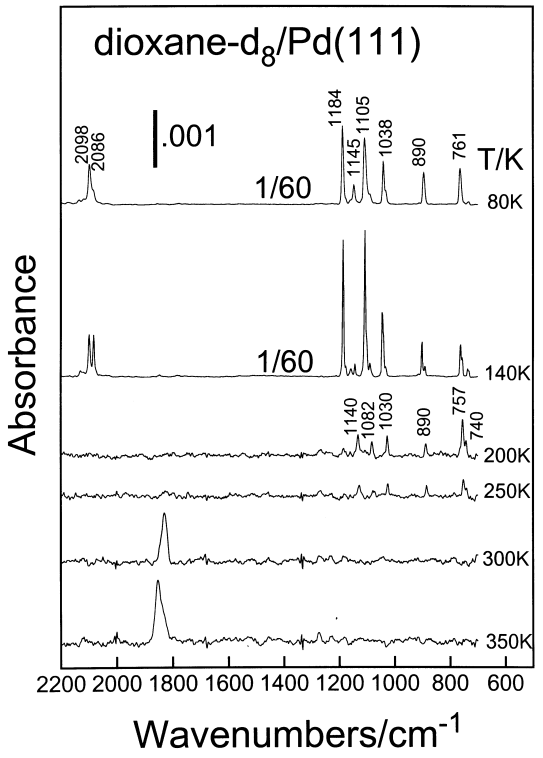

Fig. 7. Reflection–absorption infrared spectra of a multilayer of d_8-dioxane adsorbed on Pd(111) at 80 K and annealed to various temperatures. The annealing temperatures are marked adjacent to the corresponding spectrum and the absorbance scale is marked as a vertical line on the figure.

Table 1
Frequencies and assignments of the reflection–absorption infrared spectroscopy (RAIRS) spectrum collected by dosing Pd(111) with d_0-dioxane at 80 K (see Fig. 6) [38]

Frequency/cm^{-1}		Symmetry	Assignment
Gas phase	Condensed layer		
881	876	a_u	Ring stretch
889	889	b_u	CH_2 rock
1052	1050	b_u	Ring stretch
1086	1084	a_u	CH_2 rock
1136	1123	a_u	Ring stretch
1256	1258	a_u	CH_2 twist
1291	1293	b_u	CH_2 twist
1369	1367	a_u	CH_2 wag
1449	1444	a_u	CH_2 scissor
1457	1453	b_u	CH_2 scissor

Table 2
Frequencies and assignments of the RAIRS spectrum collected by dosing Pd(111) with d_8-dioxane at 80 K (see Fig. 7) [38]

Frequency/cm^{-1}		Symmetry	Assignment
Gas phase	Condensed layer		
732	–	b_u	CH_2 rock
761	761	a_u	Ring stretch
896	890	b_u	Ring stretch
1030	1038	a_u	CH_2 scissor
1118	1105	a_u	Ring stretch
1153	1145	b_u	CH_2 wag
1191	1184	a_u	CH_2 wag
2086	2086	a_u	CH_2 stretch
2098	2092	b_u	CH_2 stretch

This confirms that the low-temperature ($\sim$150 K) state is due to the desorption of a condensed multilayer, since features assigned to the multilayer have disappeared completely to leave only those additional features referred to above, although with somewhat diminished intensity. The spectra now only exhibit those features present at lower temperatures as shoulders on the main peaks. These peak positions are summarized in Table 3. Further heating to 250 K causes a further diminution in intensity of these peaks, thus confirming that the surface species that gives rise to these features desorb in the state centered at 268 K. This is further confirmed by their complete removal on

Table 3
Assignment of species formed by heating a condensed layer of d_0- or d_8-dioxane on Pd(111) to 200 K

Mode	Assignment	Frequency/cm^{-1}			
		d_0-Dioxane		d_8-Dioxane	
		Gas phase [38]	Surface	Gas phase [38]	Surface
ν_3	$CH(D)_2$ scissor	1444	1447	1225	1140
ν_4	$CH(D)_2$ wag	1397	–	1108	1082
ν_5	$CH(D)_2$ twist	1305	1300	1008	1030
ν_6	$CH(D)_2$ rock	1128	1126	832	890
ν_7	C–C stretch	1015	1043	808	
ν_8	CO stretch	837	870	752	757
ν_9	OCC deformation	435	–	490	–
			820		740

heating to 300 K, corresponding to the completion of the 268 K state. A feature that appears at $\sim$1830 cm^{-1} after annealing to 300 K is assigned to the presence of adsorbed CO [39]. This continues to grow slightly on annealing to 350 K, presumably due to the final decomposition of a small amount of remaining adsorbed dioxane present at coverages below the detection limit of our spectrometer. Further heating to $\sim$500 K leads to a featureless spectrum (not shown), corresponding to the desorption of the CO detected in the temperature-programmed desorption data in Figs. 3 and 4.

4. Discussion

Multilayers of dioxane adsorb on Pd(111) at 80 K, as evidenced by temperature-programmed desorption spectroscopy. They desorb in a relatively sharp state between 147 and 158 K, depending on exposure, and the state continues to grow in intensity with increasing exposure without saturating (Fig. 1–3). The infrared spectra confirm the presence of molecular dioxane (Figs. 6 and 7, Tables 1 and 2). Dioxane can, in principle, adopt two configurations: boat and chair [40]. There appear to be no data for the enthalpy of tautomerization of 1,4-dioxane, but the value for cyclohexane is 5–6 kcal/mol [41]. The corresponding enthalpy for 1,4-dioxane is likely to be close to, and perhaps somewhat greater than, this value. The correspondence between the gas-phase and condensed-layer infrared spectra (Tables 1 and 2) suggests that the chair conformation is maintained in the condensed layer. The multilayer is essentially completely removed by heating to 200 K, as evidenced by the temperature-programmed desorption data (Figs. 1 and 3) and the infrared spectra (Figs. 6 and 7), which show a large decrease in spectral intensity when the sample is annealed to 200 K. The resulting spectrum formed by annealing to 200 K gives rise to peaks at 1300, 1120 1043, 870 and 820 cm^{-1} following the adsorption of d_0-dioxane, and at 1140, 1082, 1030, 890, 757 and 740 cm^{-1} in the case of d_8-dioxane. Since these features decrease in intensity corresponding to the desorption of dioxane in the state centered at 268 K (Fig. 1, 3 and 4), they are assigned to the presence of intact dioxane on the surface. The activation energy for the first-order desorption of dioxane can be estimated from the Redhead equation using the experimental heating rate (7 K/s), assuming a pre-exponential factor of 1×10^{13} s^{-1}, as 16 kcal/mol [42]. This is assigned to the activation energy of desorption from a dioxane overlayer adsorbed onto the surface, since the desorption yield of the 268 K peak saturates at an exposure of $\sim$4 L (Fig. 2). This species then gives rise to infrared features that initially appear at $\sim$140 K and are uniquely present at 200 K (Figs. 6 and 7). As noted above, these features are close to the gas-phase frequencies, and this shift may be due to interaction of the adsorbate with the surface. Note, however, that the relative intensities of the peaks evident at 200 K are completely different from those for the condensed layer. If it is assumed that the condensed layer is relatively randomly oriented, the enhancements in intensities of individual features can, in principle, be exploited to determine the adsorption geometry of surface adsorbates using the surface selection rules [43]. The most prominent feature in the spectrum of d_0-dioxane after annealing to 200 K is the peak at 870 cm^{-1} (Fig. 7). Comparison with the condensed-layer spectrum of Fig. 7 following adsorption at 80 K suggests that this corresponds to the 867 cm^{-1} feature in the condensed layer (see Table 1). This is due to a ring stretching mode of a_u symmetry (Table 1). Since modes of a_u symmetry transform as the z vector in the C_{2h} point group of the chair configuration of dioxane, this suggests that the dioxane adsorbs with its z-axis relatively normal to the surface and implies a rather unphysical adsorption geometry with the C_4 plane of the dioxane oriented perpendicularly to the surface with the vector connecting the epoxide oxygen atoms oriented horizontally. In addition, other intense modes of a_u symmetry in the condensed layer, e.g. the 1123 cm^{-1} mode (Fig. 6, Table 1), which correlates with the 1120 cm^{-1} mode for the multilayer, is relatively weak. These observations suggest that dioxane no longer maintains its chair conformation in the adsorbed layer. Dioxane adsorption has been previously studied on Ag(110) and Ru(001) [36,37], where it was proposed to bond to the surface via

the lone pairs on the oxygen atoms. Such a geometry would lead to the z-axis of the molecule being oriented parallel or almost parallel to the Pd(111) surface and leading to symmetry-forbidden a_u modes; this is contrary to what is observed experimentally, where at least one vibration assigned to an a_u mode (that at 870 cm^{-1}) is very intense. An alternative possibility is that the bonding of the oxygen lone pairs to the surface is sufficiently strong that the dioxane isomerizes to the boat configuration to allow bonding of both oxygen atoms to the surface as:

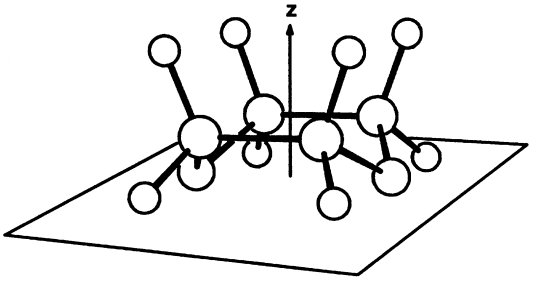

where now the z-axis of the molecule is oriented perpendicularly to the surface and the adsorbed dioxane in the boat conformation has C_{2v} symmetry. Note that a desorption state between 247 and 255 K on Ru(001) (designated the α_1 state) was proposed to be due to dioxane adsorbed with multiple O–metal bonding [37]. These values are lower than, but in the same range as, the 268 K desorption temperature found for dioxane desorption from Pd(111) (Fig. 1, 3 and 4), consistent with the geometry depicted above for dioxane on palladium.

Since the C_{2v} point group (for the boat configuration) is not a subgroup of the C_{2h} point group (of the chair configuration), it is not possible to use correlation tables to establish which irreducible representations in one point group correlate with those in the other. An alternative approach was therefore taken in which symmetry-adapted normal modes were compared for each configuration to establish which irreducible representations in the C_{2v} point group parallel those in C_{2h}. This is most easily illustrated for normal modes involving carbon–oxygen stretches: for the boat configuration (C_{2v} symmetry) the total representation decomposes into $A_1+A_2+B_1+B_2$, and for the chair configuration (C_{2h} symmetry) it decomposes into $A_g+A_u+B_g+B_u$, so that the total representation contains all possible irreducible representations in each case. The symmetry-adapted C—O modes for each of these irreducible representations for both the chair and boat conformations are displayed in Fig. 8. Comparison of the normal modes in each case allows the irreducible representations in each symmetry to be related, and these are summarized in Table 4. The surface selection rules for the proposed adsorption geometry of the boat configuration shown above indicate that only modes of A_1 symmetry should be allowed in the reflection–adsorption infrared experiment, assuming that the adsorbate maintains C_{2v} symmetry [43]. These correspond to A_g modes in the chair configuration that are symmetry forbidden in infrared spectroscopy [38]. They are, however, Raman allowed, and the frequencies of the A_g modes for gas-phase dioxane in the chair conformation obtained from the Raman spectrum are

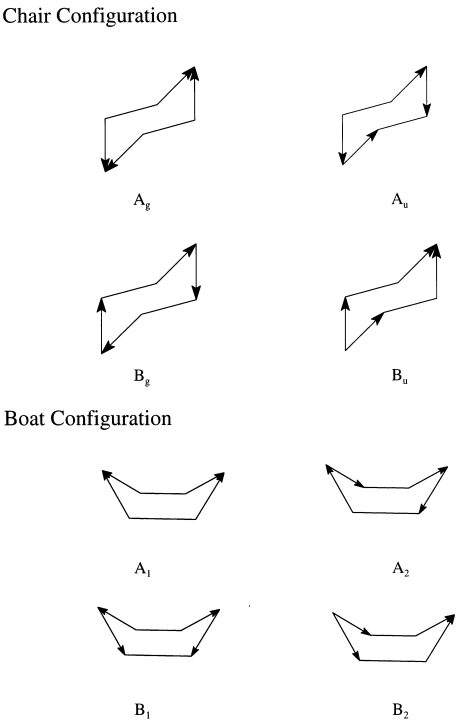

Fig. 8. Comparison of the symmetry-adapted normal modes derived from C—O stretches for dioxane in the boat and chair configurations.

Table 4
Correlation between irreducible representations for dioxane in the boat configuration (C_{2v} symmetry) with dioxane in the chair configuration (C_{2h} symmetry)

Chair configuration, C_{2h} symmetry irreducible representation	Boat configuration, C_{2v} symmetry irreducible representation
A_g	A_1
B_g	A_2
A_u	B_1
B_u	B_2

shown in Table 3 for $C_4H_8O_2$ and $C_4D_8O_2$. This also describes the nature of each of these modes. The vibrational frequencies for the normal modes in the chair and boat configurations are likely to be affected by changes in the structures of these conformers. However, the nature of the bonds and the local environments around each atom are essentially identical in the two conformers, so that the frequency differences between their corresponding normal modes are likely to be relatively small. Also shown in Table 3 are the vibrational frequencies found after annealing a condensed layer of d_0- and d_8-dioxane to 200 K. The agreement between the gas-phase and surface frequencies is extremely good, particularly for the CH_2 and CD_2 modes, which, in the proposed bonding configuration, are likely to be relatively unaffected by the presence of the surface. The CO stretching modes, at least for $C_4H_8O_2$, are perturbed by $\sim 80\ cm^{-1}$, which is consistent with bonding via the oxygen lone pairs. There remain unassigned modes at 820 cm^{-1} for d_0-dioxane and 740 cm^{-1} for d_8-dioxane. The frequency ratio of the CO stretching modes (ν_8) for perhydrogenated and perdeuterated dioxane is 1.15. The corresponding ratio for the 820 and 740 cm^{-1} modes is 1.11, suggesting that they also involve carbon–oxygen stretches.

This species desorbs from Pd(111) with a peak centered at 268 K, which a Redhead analysis suggests corresponds to a desorption activation energy of 16 kcal/mol. However, the onset of hydrogen (Fig. 5) and ethylene (Fig. 4) desorption is detected at ~ 300 K. The ethylene desorption state shows a maximum at 312 K (Fig. 4) and the hydrogen desorption state a maximum at 355 K (Fig. 5). Ethylene adsorbed on Pd(111) desorbs at ~ 300 K at low coverages [44] and hydrogen desorbs at 350 K from Pd(111) [45]. These temperatures are similar to those found for ethylene and hydrogen desorption following dioxane adsorption. This suggests that a portion of the dioxane is thermally decomposing at or below ~ 300 K. This notion is corroborated by the infrared data of Fig. 7, which confirm that adsorbed dioxane is no longer detectable on the surface at 300 K. This implies that the peak position in the dioxane desorption spectrum (Figs. 1, 3 and 4) reflects not only the desorption kinetics but also that the decrease in desorption rate at above ~ 270 K may also be due to dioxane decomposition on the surface. Certainly, a first-order desorption process should yield an asymmetric desorption state with a relatively sharp drop for the trailing edge [42], whereas the asymmetry in the experimental data is exactly opposite to this: the spectrum shows a slow decay at temperatures above 270 K. This may reflect the decomposition rather than the desorption kinetics. The thermal decomposition of dioxane at or below ~ 300 K then yields hydrogen and ethylene in the gas phase and deposits CO on the surface, as indicated by the infrared data in Figs. 6 and 7. This finally desorbs at 460 K (Fig. 3).

5. Conclusions

Dioxane adsorbs on Pd(111) to form a multilayer that desorbs at ~ 160 K to leave an overlayer, where it is proposed that dioxane adopts a boat configuration adsorbing to the surface via the lone pairs on the oxygen atoms. The dioxane desorbs with an activation energy of ~ 16 kcal/mol and thermally decomposes at or below ~ 300 K to desorb ethylene and hydrogen and deposit CO on the surface. The adsorbed CO thermally desorbs at 460 K.

References

[1] J.S. Lindsey, New J. Chem. 15 (1991) 153.
[2] C.N. Sayre, D.M. Collard, Langmuir 11 (1) (1995) 302.

[3] R.G. Nuzzo, B.R. Zegarski, E.M. Korenic, J. Phys. Chem. 96 (1992) 1355.
[4] J.P. Folkers, P.E. Laibinis, G.M. Whitesides, Langmuir 8 (5) (1992) 1330.
[5] J. Kang, P.A. Rowntree, Langmuir 12 (1996) 2813.
[6] H. Schönherr, H. Ringsdorf, Langmuir 12 (1996) 3891.
[7] H. Schönherr, H. Ringsdorf, M. Jaschke, H.-J. Butt, E. Bamberg, H. Allinson, S.D. Evans, Langmuir 12 (1996) 3898.
[8] L. Bertilsson, B. Liedberg, Langmuir 9 (1993) 141.
[9] J.T. Buontempo, S.A. Rice, S. Karaborni, J.I. Siepmann, Langmuir 9 (1993) 1604.
[10] R.G. Nuzzo, L.H. Dubois, D.L. Allara, J. Am. Chem. Soc. 112 (1990) 558.
[11] C.P. Tripp, H.L. Hair, Langmuir 11 (1) (1995) 149.
[12] H. Brunner, T. Vallant, U. Mayer, H. Hoffmann, Langmuir 12 (1996) 4614.
[13] D. Muscat, W. Kohler, Y. Geerts, Macromolecules 32 (1999) 1737.
[14] M. Weck, B. Mohr, R.H. Grubbs, J. Org. Chem. 23 (1999) 5463.
[15] C. Hamers, O. Kocian, J.F. Stoddart, Adv. Mater. 10 (1998) 1366.
[16] A.C. Try, M.M. Harding, J.K.M. Sanders, Chem. Commun. (1998) 723.
[17] C.A. Fustin, P. Rudolf, R. Caudano, Thin Solid Films 327–329 (1998) 321.
[18] S.J. Cantrill, M.C.T. Fyfe, D.J. Williams, Chem. Commun. (1999) 1251.
[19] C.J. Easton, S.F. Lincoln, H. Onagi, J. Chem. Soc. Perkins Trans. (1999) 2501.
[20] C. Seel, A.H. Parham, F. Vogtle, J. Org. Chem. 64 (1999) 7236.
[21] M.-V. Martinez-Diaz, N. Spencer, J.F. Stoddart, Angew. Chem. 36 (1997) 1904.
[22] C. Gong, H.W. Gibson, J. Am. Chem. Soc. 119 (1997) 5862.
[23] P.T. Glink, C. Schiavo, J.F. Stoddart, D.J. Williams, Chem. Commun. (1996) 1483.
[24] D.B. Amabilino, P.R. Ashton, J.F. Stoddart, Chem. Commun. (1995) 747.
[25] A. Harada, J. Lit, M. Kamachi, Nature 356 (1992) 6367.
[26] P.R. Ashton, I. Baxter, J.F. Stoddart, J. Am. Chem. Soc. 120 (1998) 2297.
[27] Y.-M. Jeon, D. Whang, K.A. Kim, Chem. Lett. (1996) 503.
[28] C.J. Pedersen, J. Am. Chem. Soc. 89 (1967) 7017.
[29] K.H. Wong, G. Konizer, J. Smid, J. Am. Chem. Soc. 92 (1970) 666.
[30] U. Takaki, T.E. Hogan Esch, J. Smid, J. Am. Chem. Soc. 93 (1971) 6760.
[31] K.M. Kemner, D.B. Hunter, W.T. Elam, P.M. Bertsch, J. Phys. Chem. 100 (1996) 11 698.
[32] W.T. Tysoe, G.L. Nyberg, R.M. Lambert, J. Chem. Soc. Chem. Commun. (1983) 623.
[33] H. Molero, B.F. Bartlett, W.T. Tysoe, J. Catal. 181 (1999) 49.
[34] G. Wu, M. Kaltchev, W.T. Tysoe, Surf. Rev. Lett. 6 (1999) 13.
[35] G. Wu, H. Molero, W.T. Tysoe, Surf. Sci. 397 (1998) 179.
[36] A. Heiland, K. Christmann, Surf. Sci. 355 (1996) 31.
[37] M.M. Walczak, P.A. Thiel, Surf. Sci. 238 (1990) 180.
[38] T. Shimanouchi, Molecular vibrational frequencies, in: W.G. Mallard, P.J. Linstrom (Eds.), NIST Chemistry WebBook, NIST Standard Reference Database Number 69, National Institute of Standards and Technology, Gaithersburg, MD 20899, 1998, http://webbook.nist.gov.
[39] A.M. Bradshaw, F.M. Hoffmann, Surf. Sci. 72 (1978) 513.
[40] F.A. Carey, R.J. Sundberg, Advanced Organic Chemistry, Plenum, New York, 1990.
[41] C.W. Beckett, K.S. Pitzer, R. Spitzer, J. Am. Chem. Soc. 69 (1947) 2488.
[42] P.A. Redhead, Vacuum 12 (1962) 203.
[43] F.M. Hoffmann, Surf. Sci. Rep. 3 (1983) 107.
[44] W.T. Tysoe, G.L. Nyberg, R.M. Lambert, J. Phys. Chem. 88 (1984) 1960.
[45] M.P. Kiskinova, G.M. Bliznakov, Surf. Sci. 123 (1982) 61.